Model of Cu-Al-Fe-Ni Bronze Crystallization

B.P. Pisarek

Department of Materials Engineering and Production Systems, Lodz University of Technology
1/15 Stefanowskiego Street 90-924 Lodz, Poland
Corresponding author. E-mail address: boguslaw.pisarek@p.lodz.pl

Abstract

According to the analysis of the current state of the knowledge shows that there is little information on the process of phase transformations that occur during the cooling Cu-Al-Fe-Ni hypo-eutectoid bronzes with additions of Cr, Mo and/or W, made additions individually or together, for the determination of: the type of crystallizing phases, crystallizing phases, order and place of their nucleation.

On the basis of recorded using thermal and derivative analysis of thermal effects phases crystallization or their systems, analysis of the microstructure formed during crystallization - observed on the metallographic specimen casting ATD10-PŁ probe, analysis of the existing phase equilibrium diagrams forming elements tested Cu-Al-Fe-Ni bronze, with additions of Cr, Mo, W and/or Si developed an original model of crystallization and phase transformation in the solid state, the casting of high quality Cu-Al-Fe-Ni bronze comprising: crystallizing type phase, crystallizing phase sequence, place of nucleation.

Keywords: Theoretical basis of foundry processes, Thermal and derivative analysis, Microstructure, Cu-Al-Fe-Ni bronze, Model of crystallization

1. Introduction

Figure 1 presents the superposition of phase equilibrium diagrams of the Cu-Al-5% Fe-5% Ni [1,2]. According to Brezina [1], eutectoid phase transformation $\beta \rightarrow \alpha + \gamma_2$ occurs at a constant temperature, and Cook et al [2] claim that this transition occurs at a temperature of TEs÷TEf (TEs-eutectoid transformation start temperature, TEf-temperature end eutectoid). The charts of these designated only one line Solvus Tκ below which nucleated and grows in bronze κ phase.

Concentration C1 marked on the chart alloy crystallizes without eutectoid transformation, and the concentration of C2 hypo-eutectoid alloy. According to [1] (Fig. 1), the process of creating a microstructure of aluminum bronze with a concentration of C1 takes place in three stages:

- β-phase crystallization directly from the liquid L (L→β),
- transformation part of the β phase in the phase α (β→α),
- κ phase separation from β phase (β→β+κ) and/or α (α→α+κ).

The process of formation of the microstructure of Al-bronze with a concentration of C2 takes place in four steps:

- β-phase crystallization directly from the liquid (L→β),
- κ phase separation from β phase (β→β+κ),
- transformation part of the β phase in the phase α (β→α),
- transformation of the remaining β phase in the eutectoid α+γ$_2$ (β→α+γ$_2$).

Further research Al-Cu-Fe-Ni bronzes revealed that the microstructure of these bronzes are identified morphologically different phases of κ [3 to 5]. For the bronze with a concentration of Al in the range described in the chart by Brezina points A÷B (Fig. 1), set the temperature of phase transitions [6]. K-phases are divided into four main types: κ$_I$, κ$_{II}$, κ$_{III}$ and κ$_{IV}$ [3÷6]. On the basis of DTA research and metallographic Brezina [3] presented a schematic form of κ-phase precipitates in alloys CuAl10Fe5Ni5 cooling down with speed of about 0.5°C/min. Brezina did not explain clearly the stage of formation of κ$_I$-phases. Its location in a typical intergrain area, on the β-phase, suggesting the possibility of crystallization of these phases of the last portion of the liquid bronze particularly enriched in admixtures of iron.
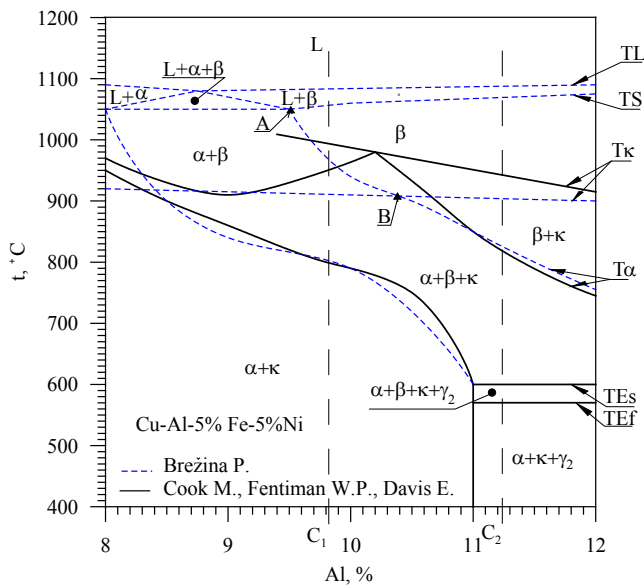
Fig. 1. Superposition of phase equilibrium diagrams
Cu-Al-5%Fe-5%Ni [1, 2]

A slightly different version of the κ-phase position presented Jahanafrooz et al [4,5] locating κ_I phase within the phase α.

The Department of Materials Engineering and Production Systems conducts research using thermal and derivative analysis (TDA) of ferro-alloys [8,9], aluminum [10,11] and copper, and especially Cu-Al-Fe-Ni hypo-eutectoid bronze with additions of Cr, Mo, W and/or C and Si [12÷15]. Only the TDA method it is possible to keep track of thermal processes of crystallization of metals and their alloys. Using the TDA method are developed computer systems of quality control liquid alloys [16].

After analyzing the current state of knowledge suggests that there is no systematic information on the process of phase transformations that occur during cooling Cu-Al-Fe-Ni hypo-eutectoid bronze with additions of Cr, Mo and/or W, made additions individually or jointly, in terms of the definition: the type of crystallizing phases, the order crystallizing phases and place of their nucleation.

2. Work methodology

Table 1 presents the range of the chemical composition of the test bronze.

Table 1.
Chemical composition of the test bronze

	Chemical composition, %							
	Al	Fe	Ni	Mn	Si	Cr	Mo	W	Cu
min.	10.38	4.43	4.50	0.3	0.02	0.01	0.00	0.00	balance
max.	10.89	4.92	5.54	0.8	0.14	0.42	0.41	0.04	

The evaluation method of thermal and derivative analysis (TDA) cooling (t=f(τ)), kinetics (dt/dτ =f '(τ)) and dynamics ($d^2t/d\tau^2$=f ''(τ)) crystallization and phase transformation in solid state of Cu-Al-Fe-Ni-(Cr, Mo, W, CrMoW) bronze was carried out using the apparatus CRYSTALDIGRAPH. Supported of a computer software for thermal and derivative analysis of alloys were determined characteristic points on the derivative curve of each sample bronze. Sample TDA curves of CuAl11Fe5Ni6 bronze shown in Figure 2. They show that the derivative curve thermal effects are the following:

Y-C-H - primary crystallization β phase
$$(L\to\beta),$$

P-Q-R - crystallization κ_{II} phase
$$(\beta\to\beta+\kappa_{II}),$$

J-K-L - partial transformation of β phase in the phase α
$$(\beta\to\beta+\alpha),$$

L-T-U - separation in the α phase, supersaturated Ni, κ_{III} phase
$$(\alpha_{(Ni)}\to\alpha+\kappa_{III}),$$

U-V-W - separation in the α phase, supersaturated Fe, κ_{IV} phase
$$(\alpha_{(Fe)}\to\alpha+\kappa_{IV}),$$

M-N-O - eutectoid transformation of the remaining β phase saturated with Al, in the eutectoid $\quad(\beta\to\alpha+\gamma_2).$

To describe the characteristic of thermal processes occurring during the primary and secondary crystallization (phase transformation in solid state) uses the following values:

- temperature of the bronze during registration characteristic points t, °C,
- the first derivative of the temperature with respect to time for these points dt/dτ, °C/s,
- the tangent of the angle of slope on the interpolated distance between characteristic points tg(α)≈$d^2t/d\tau^2$, °C/s^2,
- the time from the beginning of the measurement of characteristic points on the derivative curve (crystallization curve) τ, s.

In order to visualize the different phases in the microstructure metallographic specimens were etched with Mi20Cu reagent. The microstructure of the test specimens bronze were observed optical microscope Nikon Eclipse MA200.
To identify the chemical composition at different points of the sample cast microstructure was observed by scanning electron microscopy Hitachi scanning electron microscope S-4200 at an accelerating voltage of 25 keV, equipped with EDS analyzer.

3. Description of achieved results of own researches

3.1. Crystallization of the complex aluminum bronze

Figure 2 presents the TDA characteristics hypo-eutectoid bronze, representative of the amount made additions on the alloying elements (Table 1). Made additions alloying elements (Cr, Mo and/or W) dissolve in varying degrees in specific phases of the test bronze without affecting the change in the type of crystalliz-

ing phases and, consequently, the amount of the thermal effects of crystallization, recorded on the characteristics of TDA. Made additions alloy additives influence: the temperature t, the kinetics of dt/dτ = f '(τ) and the dynamics of Z≈d²t/dτ² thermal crystallization processes forming phase microstructure of bronze and time τ start and duration of each phase transformations occurring during primary crystallization and secondary of bronze.

The real temperature of crystallization of different phases or their system is as follows:

| liquidus (L→β)	tC	=	1082.6	°C,
solidus (β)	tH	=	1023.3	°C,
κ_{II} phase crystallization	tQ	=	897.4	°C,
α phase crystallization ($\alpha_{(Ni)}$, $\alpha_{(Fe)}$)	tK	=	812.2	°C,
κ_{III} phase crystallization $\alpha_{(Ni)} \to \alpha + \kappa_{III}$	tT	=	736.6	°C,
κ_{IV} phase crystallization $\alpha_{(Fe)} \to \alpha + \kappa_{IV}$	tV	=	702.7	°C,
eutectoid transformation $\beta_{(Al)} \to \alpha + \gamma_2$	tN	=	461.7	°C.

CuAl11Fe5Ni6 bronze microstructure in the as-cast, observed metallurgical microscope is shown in Figure 3 (a, b). It shall be composed of the phases: κ_{II}, $\alpha + \kappa_{III}$, $\alpha + \kappa_{IV}$, $\alpha + \gamma_2$. Figure 4 shows the microstructure of the test bronze observed the electron microscope. Results of chemical analysis points of the selected area, are presented in Figure 5. In the bronze CuAl11Fe5Ni6 microstruc-

ture in the as-cast, the chemical composition has been identified in the following types of phases or phase systems:κ_{II}, $\alpha + \kappa_{III}$, $\alpha + \gamma_2$. In the κ_{II} phase of the mass concentrations of individual elements have changed as follows: Fe 29.43÷66.55%, Si 3.93÷8.57%, Al 3.97÷6.87%, Ni 2.95÷4.08%, Mn 0.84÷1.72%, Cu 16.23÷54.84%. In the presented studies show that the κ_{II} phase during crystallization highly saturated elements, respectively: Fe, Si, Mn, and to a lesser extent, Al and Ni, as compared to the concentration of these elements in the alloy (Table 1).

The phases system $\alpha + \kappa_{III}$ mass concentrations of individual elements have changed as follows: Al about 9.85%, Ni 5.64÷5.92%, Fe 1.52÷1.59%, Mn 0.12÷0.33%, Si 0.14÷0.19%, Cu 82.20÷82.66%. κ_{III} phase (Ni-rich) during the crystallization phase system ($\alpha + \kappa_{III}$) strongly saturated elements, respectively: Ni and Mn, and, to a lesser extent, Fe and Si, compared to the concentration in the alloy (see Table 1). Characteristic of the system for the crystallization phase is the persistence Al concentration constant level of the order of 9.85%.

In phases system ($\alpha + \gamma_2$), the mass concentrations of the individual elements are approximately: 11.58% Al, 6.26% Ni, 1.53% Fe, 0.23% Si, 0.18% Mn, 80.21% Cu.

The characteristic of this system for the phase crystallization is the increased concentration of Al (as compared to the concentration of Al in the phase κ_{II} or phase system $\alpha + \kappa_{III}$) of about 11.58% - in conditions of equilibrium in the system Cu-Al eutectoid point is designated for the concentration of Al=11.8 %.
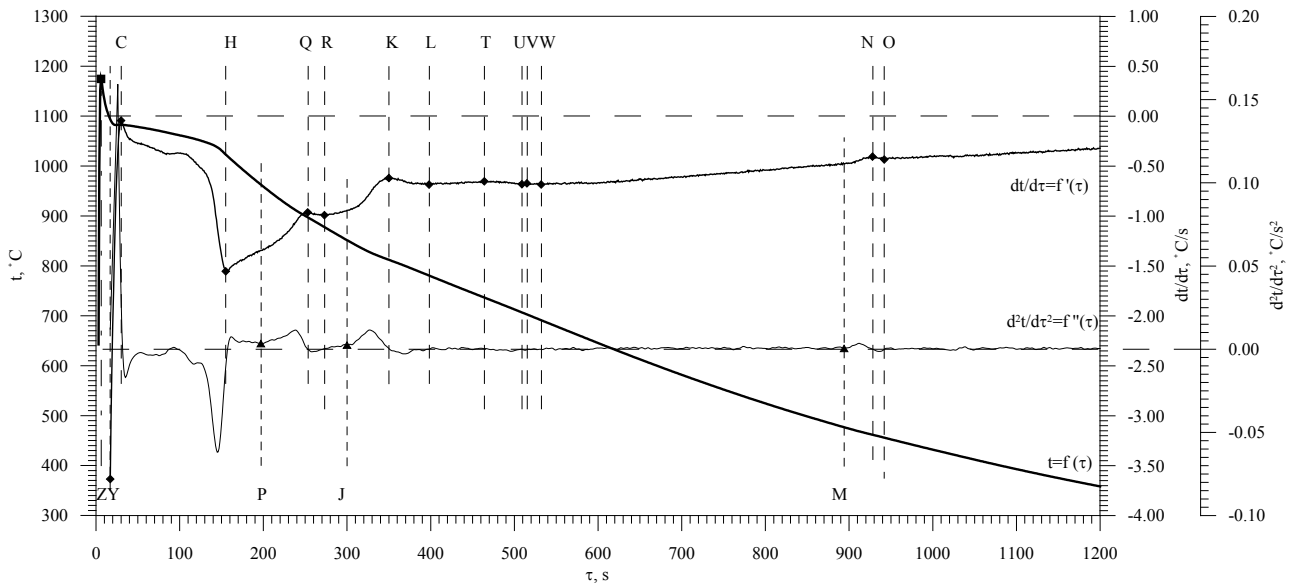
Point	Z	Y	C	H	P	Q	R	J	K	L	T	U	V	W	M	N	O
τ, s	6	17	30	155	197	253	273	300	350	398	464	509	515	532	894	928	942
t, °C	1174.7	1093.5	1082.6	1023.3	962.9	897.4	877.7	851.5	812.2	780.7	736.6	706.8	702.7	691.2	476.9	461.7	455.9
dt/dτ, °C/s	75.84	-3.63	-0.04	-1.55	-1.34	-0.96	-0.99	-0.94	-0.62	-0.68	-0.65	-0.68	-0.67	-0.68	-0.48	-0.40	-0.43
Z*10⁻³, °C/s²	-	732.49	-2.39	-63.48	10.40	-	-1.10	10.97	-	-1.08	0.35	-0.71	0.46	-0.44	3.11	-	-1.27

Fig. 2. TDA characteristics: t=f(τ), dt/dτ=f '(τ), Z≈d²t/dτ²=f ''(τ); CuAl11Fe5Ni6 bronze
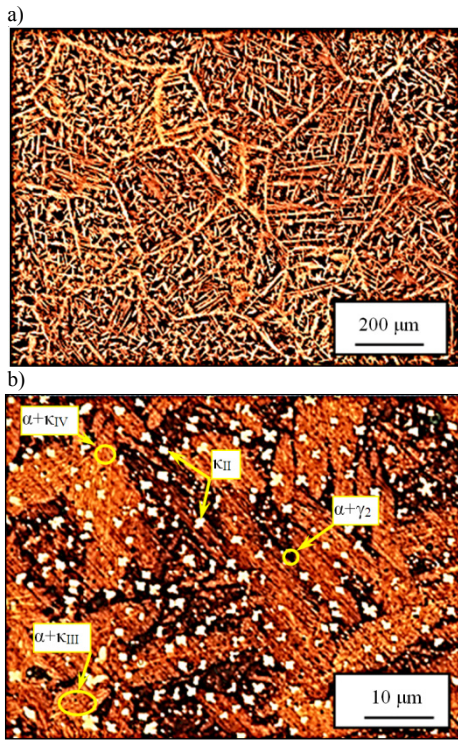
a)

b)

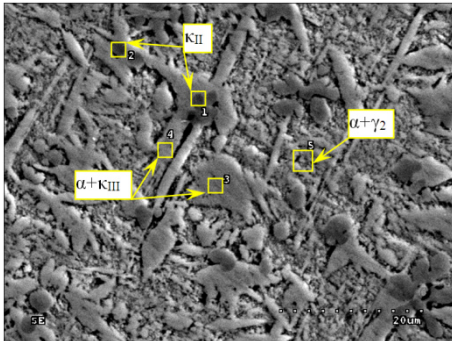Fig. 3. Microstructure of CuAl11Fe5Ni6 bronze (a, b)

Fig. 4. Microstructure of CuAl11Fe5Ni6 bronze with marked points of analysis from Scanning Electron Microscope
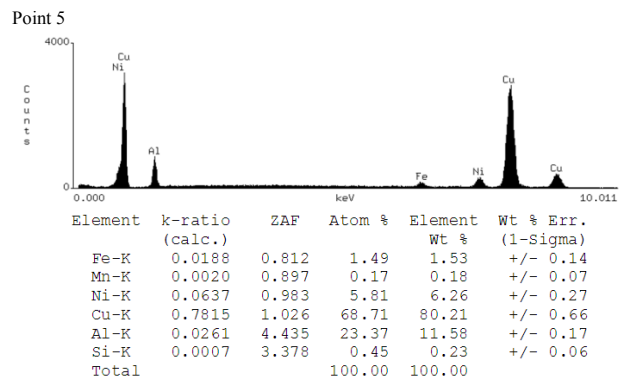
Point 1

Element	k-ratio (calc.)	ZAF	Atom %	Element Wt %	Wt % Err. (1-Sigma)
Fe-K	0.3217	0.915	28.19	29.43	+/- 0.28
Mn-K	0.0087	0.972	0.82	0.84	+/- 0.14
Ni-K	0.0389	1.050	3.72	4.08	+/- 0.25
Cu-K	0.5057	1.085	46.16	54.84	+/- 0.54
Al-K	0.0166	4.145	13.63	6.87	+/- 0.15
Si-K	0.0129	3.040	7.49	3.93	+/- 0.12
Total			100.00	100.00	

Point 2

Element	k-ratio (calc.)	ZAF	Atom %	Element Wt %	Wt % Err. (1-Sigma)
Fe-K	0.6681	0.996	60.15	66.55	+/- 0.47
Mn-K	0.0167	1.032	1.58	1.72	+/- 0.19
Ni-K	0.0257	1.148	2.54	2.95	+/- 0.30
Cu-K	0.1386	1.171	12.89	16.23	+/- 0.45
Al-K	0.0109	3.638	7.43	3.97	+/- 0.14
Si-K	0.0326	2.630	15.40	8.57	+/- 0.16
Total			100.00	100.00	

Point 3

Element	k-ratio (calc.)	ZAF	Atom %	Element Wt %	Wt % Err. (1-Sigma)
Fe-K	0.0197	0.807	1.58	1.59	+/- 0.13
Mn-K	0.0013	0.892	0.12	0.12	+/- 0.06
Ni-K	0.0576	0.980	5.35	5.64	+/- 0.25
Cu-K	0.8080	1.023	72.37	82.66	+/- 0.62
Al-K	0.0219	4.506	20.31	9.85	+/- 0.15
Si-K	0.0004	3.365	0.27	0.14	+/- 0.05
Total			100.00	100.00	

Point 4

Element	k-ratio (calc.)	ZAF	Atom %	Element Wt %	Wt % Err. (1-Sigma)
Fe-K	0.0188	0.807	1.51	1.52	+/- 0.15
Mn-K	0.0037	0.892	0.33	0.33	+/- 0.07
Ni-K	0.0604	0.980	5.60	5.92	+/- 0.27
Cu-K	0.8031	1.023	71.90	82.20	+/- 0.68
Al-K	0.0219	4.501	20.29	9.85	+/- 0.16
Si-K	0.0006	3.362	0.37	0.19	+/- 0.06
Total			100.00	100.00	

Point 5

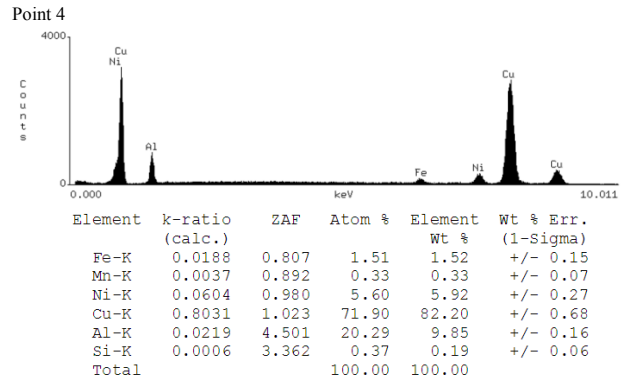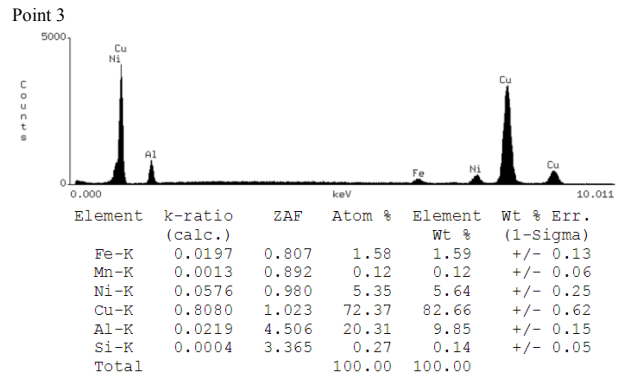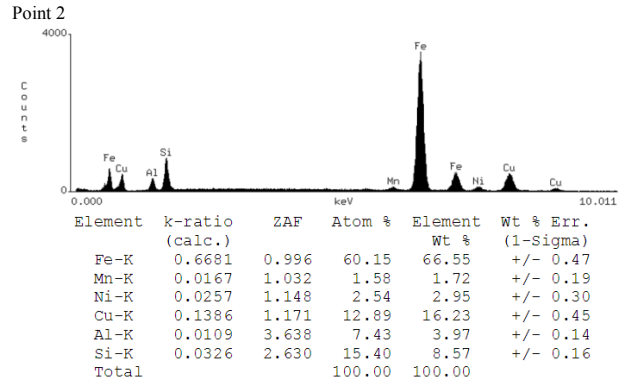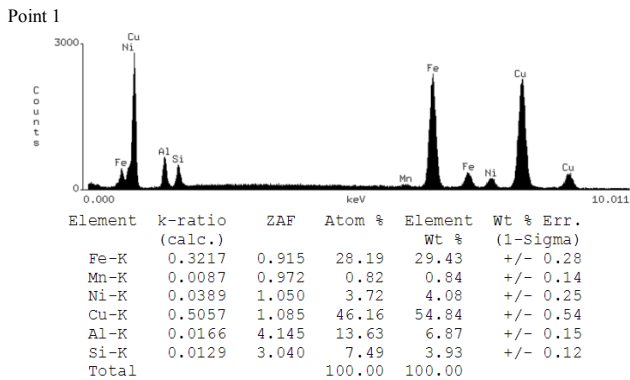| Element	k-ratio (calc.)	ZAF	Atom %	Element Wt %	Wt % Err. (1-Sigma)
Fe-K	0.0188	0.812	1.49	1.53	+/- 0.14
Mn-K	0.0020	0.897	0.17	0.18	+/- 0.07
Ni-K	0.0637	0.983	5.81	6.26	+/- 0.27
Cu-K	0.7815	1.026	68.71	80.21	+/- 0.66
Al-K	0.0261	4.435	23.37	11.58	+/- 0.17
Si-K	0.0007	3.378	0.45	0.23	+/- 0.06
Total			100.00	100.00	

Fig. 5. Charts analysis and the results of the chemical composition at points 1 to 5 microstructure of CuAl11Fe5Ni6 bronze, solidifying in the ATD10-PŁ sampler

3.2. Model of aluminum bronze crystallization

A graphic model of crystallization and phase transformation in solid Cu-Al-Fe-Ni bronzes hypo-eutectoid no intermetallic phases MM_X type (where X={Mo, W, Cr, MoWCr}) and κ_I is shown in Figure 6. This process is divided into stages I to VIII, in relation to the characteristic points that define the temperature of phase transformation in bronze, appointed by TDA method. After pouring bronze into the mould, the molten alloy is cools and transfer to its superheat (Stage I). After the alloy supercooling below the equilibrium liquidus temperature TL (Stage II), in liquid form on the walls of the mold and on the precipitate particles (the undissolved solid phase) contained in the bronze, nucleates β phase and grows, up to the solidus temperature TS. In the range of solidus temperature TS and solvus Tκ (Tκ_{II}) alloy cools a single-phase (Stage III), with a non-equilibrium concentration of admixtures in grains of β phase. After supercooling bronze below the equilibrium Tκ solvus temperature, on the interphase boundaries and within the β phase, in areas rich in Fe, nucleates and grows in the form of "rosettes", to the Tα solvus temperature, intermetallic κ_{II} phase rich in iron and aluminum and high-melting alloy additions (Cr, Mo, W, Si) (Stage IV). After supercooling bronze below the equilibrium solvus Tα temperature, as a result of the increase in the solubility Al in the phase β, Al is diffusing from the phase boundary inwards grains of the phase β, and dealuminize the layer of the β phase is changing into the phase α, forming the outline of the primary β phase (V_s Stage, s-start, beginning of the β → β+α transformation). Next, this process cover the inside of the β phase. Nucleation and growth in the form of plates or "narrow lens", richer in alloying additives α phase, started in various places on the previously crystallized the α phase on interphase boundaries. Phase α may also nucleate close to κ_{II} phase precipitates, that during the nucleation and growth parent β phase impoverished its not only high melting bronze admixtures, but also of aluminum. Hence also, impoverished into admixtures alloy and aluminium phase β, transforms, along with a fall in temperature, into the phase α, with non-equilibrium concentration of admixtures. The excess aluminum in the increasing α phase, is relegated to β phase, by diffusion, to the front of its crystallization. Al-rich phase β is trapped in a small area between the plates and lens α phase (Stage V_f, f-finish, the end of the transformation β→β+α). After supercooling bronze, below the equilibrium Tκ_{III} solvus temperature inside platelets or lenticular α phase precipitates, saturated nickel (α(Ni)), nucleate and grows κ_{III} intermetallic phase, rich in Ni and high-melting alloying elements (Cr, Mo, W, Si). Nucleation and growth phases κ_{III} characterized by a certain analogy to the process of formation of pearlite in iron alloys. Nonequilibrium phase transformation of α phase, saturated Ni and alloying elements in the system of phases α+κ_{III}, starts from the nucleation κ_{III} phase in a plates. Growing the plate κ_{III} phase, impoverishes α phase in admixtures, hence next lamellar κ_{III} phase separation are separated lanes α phase poor in alloy additives (Stage VI). In the α phase, poorer in Ni and the alloying elements, but richer in Fe (α(Fe)), after the supercooling below the equilibrium Tκ_{IV} solvus temperature, due to the decreasing solubility of Fe and of the alloying admixtures in this phase, nucleates and grows in the form of spheroidal precipitates intermetallic κ_{IV} phase, rich in Fe and alloying elements (Stage VII). The form of κ_{IV} phase precipitates is probably due to

the fact, that precipitates of this phase takes place already at relatively low temperatures and diffusion of admixtures in the α phase may occur at a relatively short distance. After supercooling bronze below the TE equilibrium eutectoid temperature, the rest of the phase β (β (Al)), which has not been changed to α phase due to the high content of Al, transforms into the eutectoid α+γ_2 (Stage VIII).

As a result of the primary and secondary crystallization (phase transformation in solid state) in the microstructure bronze formed phase microstructure consisting of: κ_{II}+(α+κ_{III})+(α+κ_{IV})+(α+γ_2).

Phase transformation and the transformation temperature range during cooling in the ATD10-PŁ sampler bronzes Cu-Al-Fe-Ni with limited additions of Cr, Mo, W and/or Si (Table 1) shown in Figure 7. Due to the fact that the cooling process of bronze in the sampler ATD10-PŁ occurs at a faster rate than in the conditions of equilibrium (which generates bigger supercooling in crystallization process) must be assumed, that the equilibrium crystallization temperature and phase transformation in the solid state are relatively slightly higher than the set ATD method in the sampler.
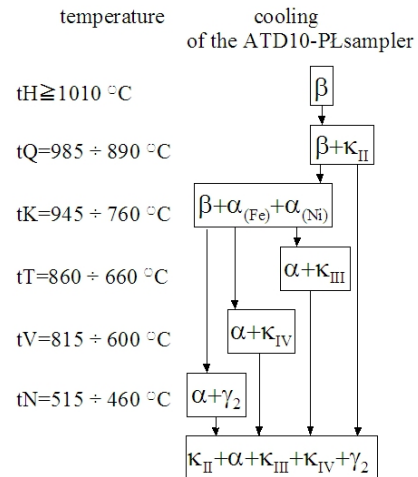

Fig. 7. Phase transformation during cooling Cu-Al-Fe-Ni bronzes with limited additions of Cr, Mo, W and/or Si

4. Conclusions

The following conclusions result from the presented study:
- elaborated model of crystallization and phase transformation in the solid state hypo-eutectoid Cu-Al-Fe-Ni bronze, crystallize without a MM_X intermetallic phases (where X = {Mo, W, Cr, MoWCr}) and κ_I defines:
  - the type of crystallizing phases,
  - the order of crystallizing phases,
  - the place of nucleation,
- studies it possible to determine the actual temperature ranges of phase transformations in Cu-Al-Fe-Ni bronze with low quantity of additions of Cr, Mo, W and/or Si,
- knowledge of the actual temperature ranges of phase transformations in the studied bronzes, allows you to control the microstructure of the bronze after heat treatment.
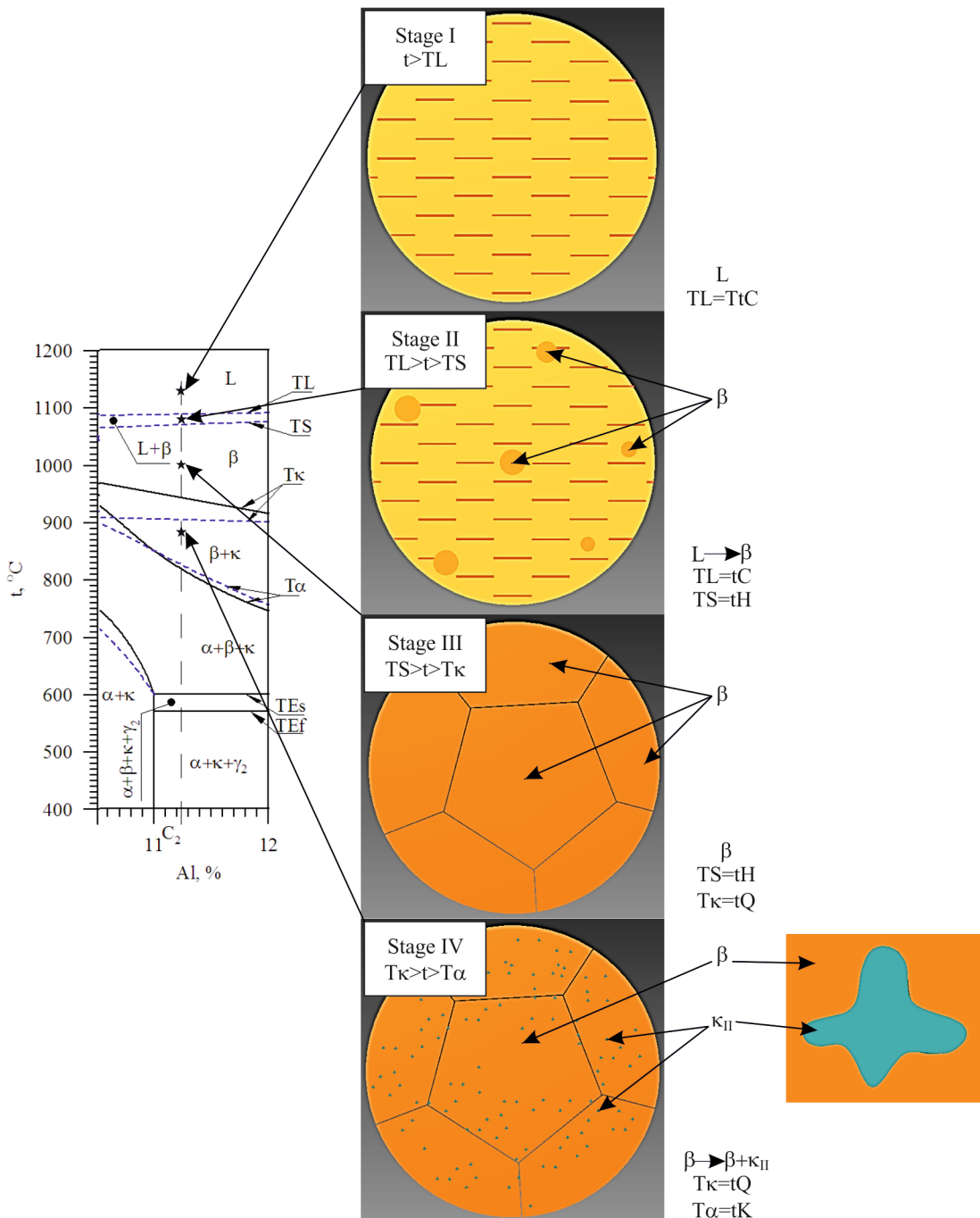
Fig. 6. The Model of crystallization and phase transformation in the solid state hypo-eutectoid Cu-Al-Fe-Ni bronzes without intermetallic phases type of a MM_X (where X={Mo,W,Cr,MoWCr}) and κ_I
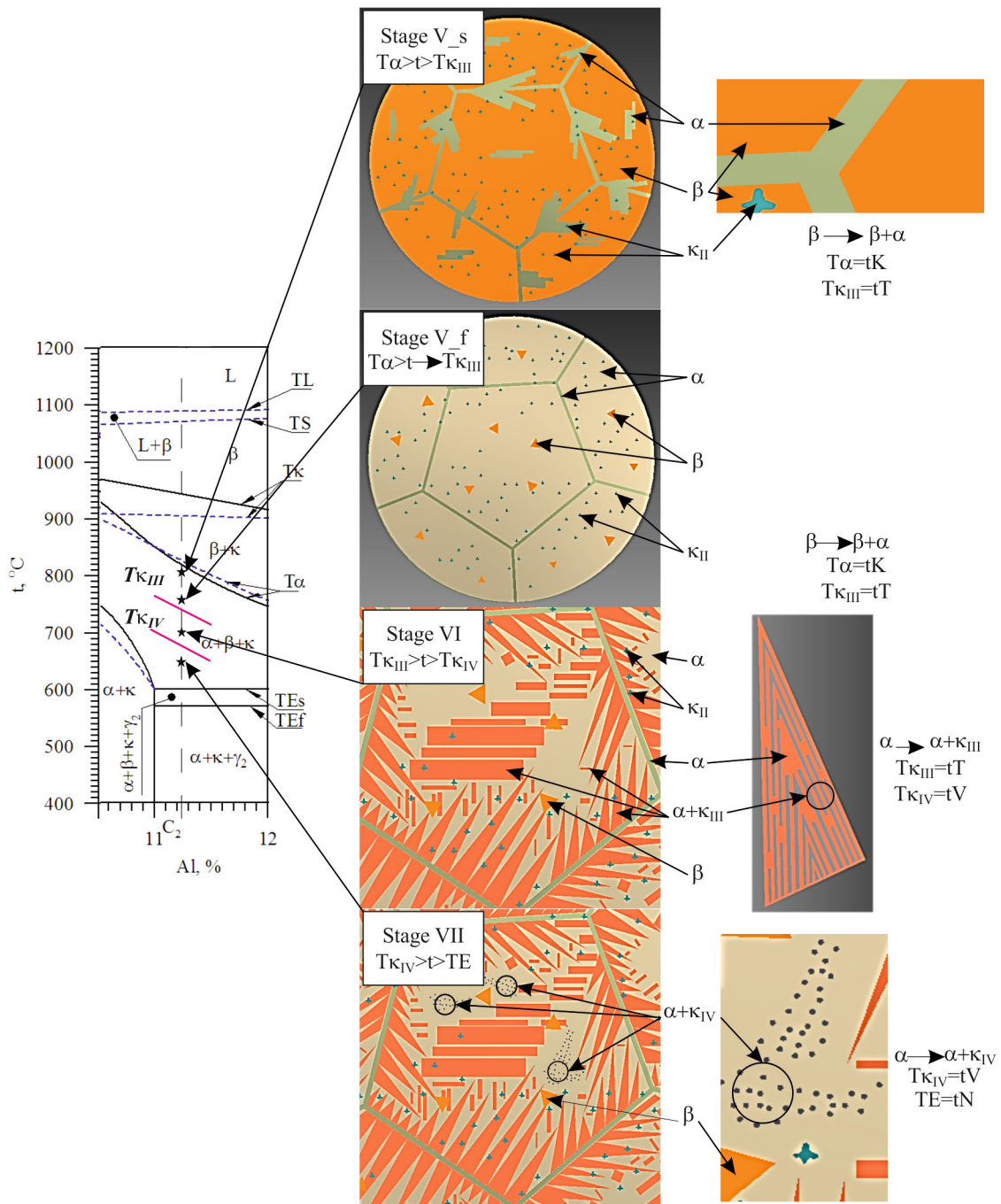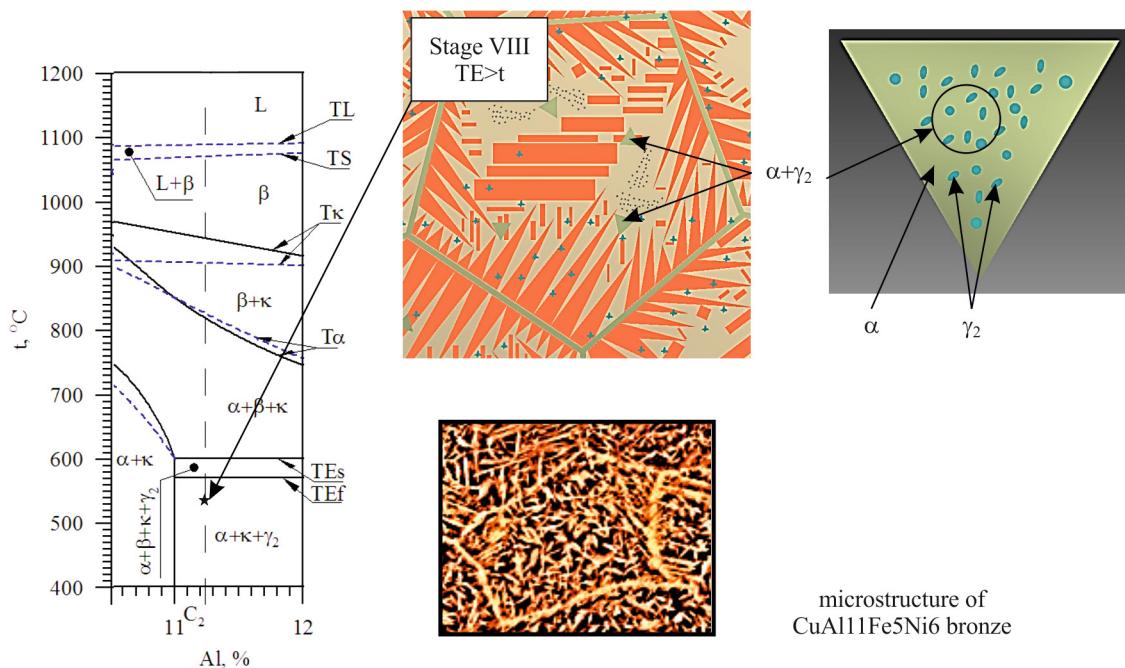
Fig. 6. (cont.) The model of crystallization and phase transformation in the solid state hypo-eutectoid Cu-Al-Fe-Ni bronzes without intermetallic phases type of a MM_X (where X={Mo,W,Cr,MoWCr}) and κ_I

Fig. 6. (cont.) The model of crystallization and phase transformation in the solid state hypo-eutectoid Cu-Al-Fe-Ni bronzes without intermetallic phases type of a MM_X (where X={Mo,W,Cr,MoWCr}) and κ_I

Acknowledgements

References

[1] Brezina, P. (1973). Gefügeumwandlungen und mechanische Eigenschaften der Mehrstoff-Aluminiumbronzen vom Typ CuAl10 Fe5 Ni5. *Giesserei-Forschung*. 25(3), 1-10.

[2] Cook, M., Fentimen, W.P. & Davis, E. (1951-52). Observations on the structure and properties of wrought cooper-aluminium-nickel-iron alloys, *J. Inst. Metals*. 80, 419/29.

[3] Brezina, P. (1973). Gefögeumwandlungen und mechanische Eigenschaften der Mehrstoff-Aluminiumbronzen vom Typ Cu-Al 10 Fe5 Ni5. *Giesserei-Forschung,* 25(3), 1-10.

[4] Hasan, F., Jahanafrooz, A., Lorimer, G.W. & Ridley, N. (1982). The Morphology, Crystallography, and Chemistry of Phases in As-Cast Nickel-Aluminum Bronze. *Met. Trans A*. 13a, 1337-1345.

[5] Jahanafrooz, A., Hasan, F., Lorimer, G.W. & Ridley, N. (1983). Microstructural Development in Complex Nickel-Aluminum Bronze. *Met. Trans A*. 14a, 1951-1956.

[6] Fuller, M.D. (2006). *Friction Stir Processing and Fusion Welding in Nickel Aluminum Propeller Bronze*. Thesis, Thesis Advisor: Terry R. McNelley, Naval Postgraduate School, Monterey, California, USA.

[7] Weill-Couly, P. & Arnaud, D. (1973). Influence De La Composition Et De La Structure Des Cupro-Aluminiums Sur Leur Comportment En Service. *Fonderie*. 322, 123-135.

[8] Gumienny, G. (2011). TDA method application to austenite transformation in nodular cast iron with carbides assessment. *Archives of Foundry Engineering*. 11(3), 159-166.

[9] Gumienny, G. (2010). Bainitic-martensitic nodular cast iron with carbides. *Archives of Foundry Engineering*. 10(2), 63-68.

[10] Pietrowski, S. & Szymczak, T. (2009). Silumins alloy crystallization. *Archives of Foundry Engineering*. 9(3), 143-158.

[11] Pietrowski S. & Szymczak, T. (2010). Crystallization, micro-structure and mechanical properties of silumins with micro-additions of Cr, Mo, W and V. *Archives of Foundry Engineering*. 10(1), 123-136.

[12] Pisarek, B. (2007). The crystallization of the bronze with additions of Si, Cr, Mo and/or W. *Archives of Materials Science and Engineering*. 28(8), 461-466.

[13] Pisarek, B. (2010). Influence of the technology of melting and inoculation preliminary alloy AlBe5 on change of concentration of Al and microstructure of the bronze CuAl10Ni5Fe4. *Archives of Foundry Engineering*. 10(2), 127-134.

[14] Pisarek, B. (2011). Effect of additions Cr, Mo, W and/or Si on the technological properties on the technological properties of aluminium-iron-nickel bronze. *Archives of Foundry Engineering*. 11(3), 199-208.

[15] Pisarek, B. (2012). Effect of annealing time for quenching CuAl7Fe5Ni5W2Si2 bronze on the microstructure and mechanical properties. *Archives of Foundry Engineering*. 12(2), 187-204.

[16] Pietrowski, S. & Pisarek, B. (2007). Computer-aided technology of melting high-quality metal alloys. *Archives of Metallurgy and Materials*. 52(3), 481-486.